JMEPEG (2011) 20:1346–1354
DOI: 10.1007/s11665-010-9733-y

1059-9495/$19.00

Influence of Annealing Heat Treatment and Cr, Mg, and Ti Alloying on the Mechanical Properties of High-Silicon Cast Iron

D.B.V. Castro, L.S. Rossino, A.M.S. Malafaia, M. Angeloni, and O. Maluf

(Submitted May 13, 2009; in revised form July 16, 2010)

The influence of annealing on the mechanical properties of high-silicon cast iron for three alloys with distinct chromium levels was investigated. Each alloy was melted either with or without the addition of Ti and Mg. These changes in the chemical composition and heat treatment aimed to improve the material's mechanical properties by inhibiting the formation of large columnar crystals, netlike laminae, precipitation of coarse packs of graphite, changing the length and morphology of graphite, and rounding the extremities of the flakes to minimize the stress concentration. For alloys with 0.07 wt.% Cr, the annealing reduced the impact resistance and tensile strength due to an enhanced precipitation of refined carbides and the formation of interdendritic complex nets. Annealing the alloys containing Ti and Mg led to a decrease in the mechanical strength and an increase in the toughness. Alloys containing approximately 2 wt.% Cr achieved better mechanical properties as compared to the original alloy. However, with the addition of Ti and Mg to alloys containing 2% Cr, the chromium carbide formation was inhibited, impairing the mechanical properties. In the third alloy, with 3.5 wt.% of Cr additions, the mechanical strength improved. The annealing promoted a decrease in both hardness and amount of iron and silicon complex carbides. However, it led to a chromium carbide formation, which influenced the mechanical characteristics of the matrix of the studied material.

Keywords annealing, cast iron, chromium, high silicon, mechanical properties

1. Introduction

High-silicon cast irons are basically ternary Fe-C-Si alloys recommended for applications to which high corrosion resistance is required (Ref 1-10). Such characteristic is achieved due to the formation of a protective coating of hydrated silicon oxide on the material's surface (Ref 1). This corrosion resistance is improved as the amount of silicon increases, reaching the best results in the 14.20-14.75 wt.% range of this element (Ref 2). However, the mechanical properties are proportionally damaged as the amount of silicon is increased. A commercial alloy with approximately 15.0 wt.% of silicon at room temperature presents low mechanical strength, i.e., around half of that presented by a high-quality gray cast iron (Ref 3). This low mechanical strength can be explained by the presence of Fe + Fe_3Si_2 + C carbides and graphite precipitated in coarse form and Fe + Fe_3Si_2 in solid solution (Ref 1). Therefore, the use this alloy is limited to situations in which mainly corrosion and wear resistance is required. Another difficulty of the studied alloys is their high hardness (480-520 HB), thus they can only be slowly machined with special tools. Since drilling and screwing operations are impossible to perform, the problem can be solved by inserting ductile metals in the piece mold (Ref 1-5).

Concerning silicon in cast irons, it affects the occurrence, properties, and distribution of constituents in the microstructure, when added above 3 wt.%; due to its stabilizing ferrite properties, it promotes a carbon decrease in the eutectic composition and favors graphite formation during the solidification process (Ref 3). In cast irons with 14-17 wt.% silicon, the ferritic matrix is saturated by silicon and contains very small graphite flakes (carbon between 0.4 and 1.0 wt.%), as the silicon promotes ferrite (Ref 2, 6).

The increase in the carbon level decreases the tensile strength of the high-silicon cast iron (Ref 3). Riley et al. (Ref 7) presented an approximation of a phase diagram in the plain section of a ternary diagram shows some common defects caused by different carbon contents between 0.30 and 0.90 wt.%; the other main alloy elements in this diagram were 15 wt.% Si and 0.65 wt.% Mn (Ref 7). An important particularity of high-silicon iron is the smaller amount of carbon in the eutectic composition (around 0.8 wt.%) than gray cast iron. Hurst (Ref 8) presented three different high-silicon iron microstructures: eutectic, hypo, and hypereutectic. The hypoeutectic and eutectic alloys showed a type of fine graphite in the microstructure, and although the hypereutectic alloy contained fine graphite, it also had primary graphite in flakes. To avoid coarse graphite formation, the author suggested that alloy should be agitated during solidification, resulting in a material with smaller graphite flakes in the length.

D.B.V. Castro, L.S. Rossino, A.M.S. Malafaia, M. Angeloni, and **O. Maluf**, Materials, Aeronautics and Automotive Engineering Department, Engineering School of São Carlos, University of São Paulo, São Carlos, SP, Brazil. Contact e-mail: danilobvc@yahoo.com.br.

Chromium is an alloying element used to increase the corrosion strength and stabilize the structure for high-temperature applications in cast irons. It is the most effective element to improve the resistance at high temperatures and protect against oxidation, as it stabilizes the iron carbide decreasing the probability of rupture at high temperatures. For temperatures above 760 °C, 5.5 wt.% Cr content reaches oxidation resistance to cast iron (Ref 3). In high-silicon iron, 3-5 wt.% Cr are recommended to improve the corrosion resistance in environments containing hydrofluoric and hydrochloric acids (Ref 2).

Magnesium has been reported as an inoculant to prevent the formation of flake graphite in cast irons, forming a nodular or spheroidal graphite structure. In nodular cast iron, the Mg content generally ranges from 0.005 to 0.2% and promotes desirable ductile qualities to the iron (Ref 11-13). On the other hand, the formation of MgS sulfides causes higher corrodibility in nodular cast irons (Ref 13). Titanium is added to the gray cast iron to increase strength and improve wear resistance, due to the friction coefficient decrease caused and the presence of hard titanium carbides (Ref 14, 15). Molybdenum is used in high-silicon cast iron to allow corrosion resistance in environments of hydrochloric and hydrofluoric acids (Ref 1, 2, 4, 6, 8, 9). However, regarding nitric acid, molybdenum does not present any improvement, sometimes causing a decrease in the corrosion resistance (Ref 10).

One of the major problems in the production of high-silicon cast iron is the defects related to gases. During casting, the molten metal shows a propensity to absorb gases, which increases with overheating. By the vacuum melting process, it is clearly defined that the porosities are caused mainly by CO and H_2. Therefore, moisture must be avoided during the whole process in the metallic charge, coating or repair of the furnace, ladle refractory, or sand mold. Another factor of high importance in the studies of high-silicon cast iron properties is the melting temperature. It has been observed that, at temperatures higher than the ones recommended, there is a tendency to form columnar crystals. On the other hand, for temperatures below those recommended there occurs the formation of very fine particles. According to Fig. 1, the best temperature range must be between 1220 and 1280 °C, depending on the carbon level and the piece's thickness and geometry (Ref 7, 8).

An evaluation of the pouring temperature, casting temperature, and mischmetal addition was performed in a 14.5 wt.% Si high-silicon iron. Regarding pouring temperature, the tensile results showed that specimens poured at 1350 °C obtained better results than those poured at 1430 °C. This behavior was justified by the hydrogen solubility decrease at the lowest temperatures. To evaluate the metal cast temperature effect, temperatures of 1550 and 1650 °C were used. The best results were achieved at higher temperatures, as the SiO_2 oxide formation is inhibited, and at lower temperatures its formation is more stable than CO, causing oxidized specimens (Ref 4). The addition of 0.2 wt.% mischmetal (rare earth) was effective to the material degasification and microstructure refinement. The improvement could be perceived in the tensile and corrosion resistances and justified by the porosity decrease and primary ferrite increase (Ref 4). The use of cerium, one of the elements of mischmetal, caused the same improvement in high-silicon irons (Ref 1).

As the solidification contraction of high-silicon cast iron (1.7%) is higher than the ordinary gray cast iron (1.0%), the mold and core projects must be studied carefully. The molds must be conceived in such a way that they can support the pressure of liquid material, but they need to collapse at the correct time. After pouring, the molds and cores must be broken and the pieces must be sent directly to the furnace under

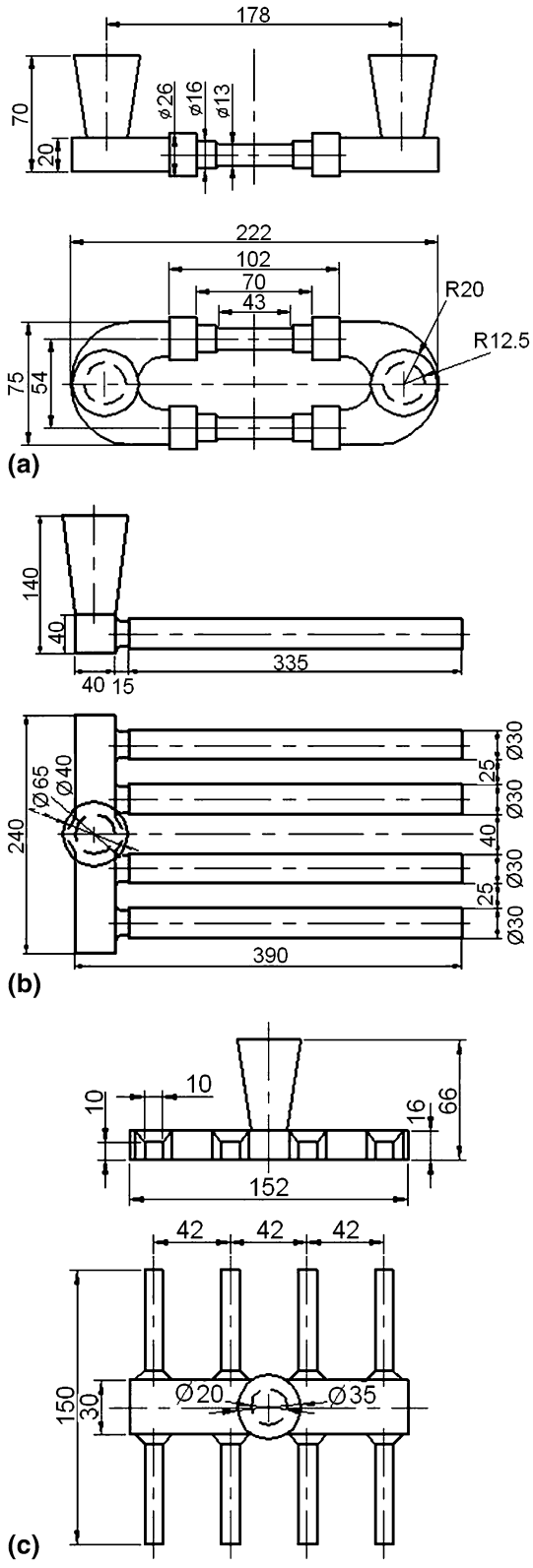

Fig. 1 Schematic diagrams of the dispositions of test specimens and feed pouring gates in: (a) tensile, (b) bending, and (c) impact foundry patterns (dimensions in millimeters)

annealing temperature (Ref 8). The experimental data showed that, at temperatures higher than 700 °C, the high-silicon cast iron had a higher degree of hardness and plasticity when compared to its properties at room temperature. The mechanical strength of these cast irons at these temperatures allows a safe handling during the stripping. On the other hand, at temperatures higher than 800 °C, excessive ductility leads to deformation. The annealing temperature must not exceed this temperature, and the annealing time is determined by the thickness of the cast part. The cooling must be slow and performed inside the furnace, allowing the material to relieve the strain that causes cracks during the phase transformation. The thermal treatment is an attempt to decompose and distribute carbides and homogenize the microstructure (Ref 8).

This study aims to evaluate the effect of chromium, titanium, and magnesium and the annealing treatment on the mechanical properties of a high-silicon iron. All modifications in the alloys were made to improve the material's tenacity. Twelve alloys were evaluated: with three different chromium contents, with or without titanium and magnesium, and with or without annealing. In this manner, all parameters could be observed, helping to understand the individual effects on the microstructure and mechanical properties.

2. Materials and Methods

2.1 Studied Alloys

Three types of high-silicon cast iron alloys were studied, as shown in Table 1. The chemical compositions were based on the ASTM A-518M-99 standard (Ref 16). The addition of alloying elements, such as magnesium, titanium, and molybdenum, aimed to increase the mechanical strength, as for brittle materials such as high-silicon iron, the tenacity is improved with an increase in the strength. Mg was added to decrease the stress concentration caused by the sharp tips of graphite, due to the Mg property of rounding the graphite tips. The Ti addition aimed to precipitate titanium carbides dispersed in the matrix to improve the alloy strength, and consequently the alloy tenacity. Molybdenum was added to all alloys to raise the hot mechanical strength. The denomination "*" indicates that titanium and magnesium were added to the alloys during the casting process.

2.2 Foundry Patterns and Molding

The foundry patterns used in this study were prepared to allow different types of test specimens (tensile, impact, and bending). They were fabricated with dimensions as close as the final dimensions of the parts to allow an easily separation from the respective pouring gates. The molds were handmade and sealed right before pouring. The block drawings along with their respective pouring gates, hot top and dimensions (in millimeters) are shown in Fig. 1.

The molding system used for the test specimen was synthetic sand (green), which is composed basically of a mix of quartzous sand (78 wt.%), sodic bentonite (montmorillonite 10 wt.%), pulverized coal, Cardiff (8 wt.%), and water (4 wt.%). This type of molding was adopted as it is the one that best fits the molding project requirements for high-silicon cast iron. It presents low resistance during the solidification contraction, thus avoiding the cracking of the casting part.

The test specimen molding operation was handmade in the foundry laboratory with sand prepared in an Eirich-type conventional mixer, with capacity of 100 kg per load. The respective patterns and expansive wood molding boxes were used so that they were open in every operation and allowed withdrawing the mold cake. To avoid possibility of defects caused by H, a less humidity content was used in the molds.

2.3 Fusion, Pouring, Stripping, and Heat Treatment

The metallic loads used were AISI 1020 steel, ferro-silicon (75% of Si), ferro-chromium (50% of Cr), ferro-titanium (27% of Ti), ferro-molybdenum (65% of Mo), ferro-manganese (70% of Mn), ferro-silicon-magnesium (7% of Mg), and graphite. The casting of the metallic loads was made in a Inductotherm induction furnace, with 50 kW power, 3200 Hz frequency, and a crucible of 30 kg capacity made of silicon carbide and coated with aluminous refractory (Morganite brand, model AS13), at the foundry laboratory of DEMA (Materials Engineering Department) of UFSCar (Federal University of São Carlos). The temperature standard measurements were taken with an Ecil immersion pyrometer model Eciltemp.

Before pouring, the last element added to the metallic bath was ferro-titanium. During the transference, after the cleaning and the temperature checking, an inoculation with ferro-silicon-magnesium was made in the liquid metal jet from the furnace to the foundry ladle to increase the number of nucleation by product and refine the granulometry. The pouring temperature was always the lowest as possible, in a range from 1250 to 1300 °C.

The annealing heat treatment was performed in a Gallenhamp furnace. After pouring, half of the cast specimens, with their pouring gates, were transferred to a heat treatment furnace stabilized at 800 °C. The permanency time used was 1 h/mL of the test specimen thickness. The test specimens were cooled until room temperature, using a controlled rate (about 150 °C/h). The other half was cooled inside the molds until it reached room temperature, and then stripped.

All test specimens, annealed or not, reached room temperature, were cleaned and the pouring gates and rough edges were removed.

Table 1 Factual chemical composition of high-silicon cast iron alloys (wt.%)

Elements	C	Si	Mn	P	S	Cr	Mo	Cu	Ti	Mg
C1	0.66	14.40	0.31	0.013	0.018	0.07	0.17	0.40	0.006	-
C2	0.76	14.37	0.40	0.014	0.009	2.51	0.23	0.39	0.009	0.001
C3	0.63	14.50	0.34	0.021	0.016	3.66	0.26	0.38	0.008	-
C1*	0.68	14.47	0.43	0.017	0.014	0.07	0.28	0.42	0.180	0.014
C2*	0.67	14.32	0.39	0.012	0.010	1.96	0.38	0.49	0.120	0.014
C3*	0.65	14.16	0.36	0.017	0.010	3.81	0.39	0.42	0.150	0.015

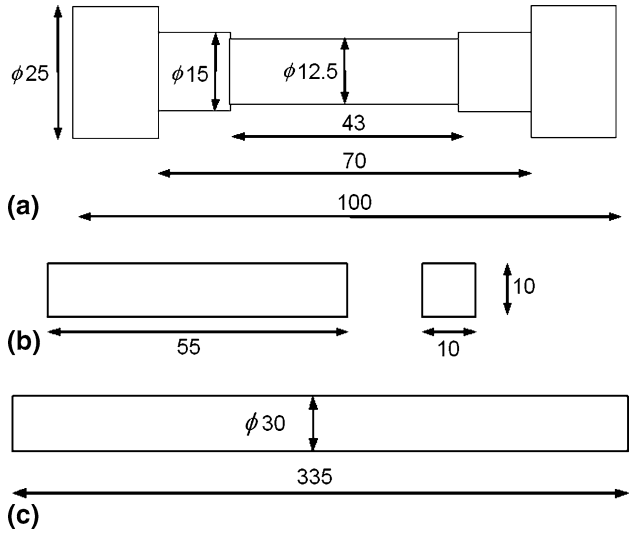

Fig. 2 Test specimens used in the mechanical tests: (a) tensile, (b) impact, and (c) bending (dimensions in millimeters)

2.4 Mechanical tests

The tensile tests of the high-silicon cast iron specimens (annealed and as-cast) were performed at room temperature at load rate of 1 mm/min, using a 10 kN load cell, EMIC brand, model DL 10000, automated and equipped with Tesc software and used for data retrieving. The test specimens used for the tests are shown in Fig. 2(a) and comply with ASTM E-8M standards. The results of tensile strength—σ_u—for each studied compound were acquired by arithmetic mean from the specimens results (four specimens) of each compound.

The Charpy specimens were made without notch and tested at room temperature in an Instron Wolpert machine, model PW30. The test specimens were shaped according to ASTM E-23 standards, as shown in Fig. 2(b). The results of absorbed energy during the Charpy tests are the average taken in five measurements performed in the specimens for each studied alloy.

Bending tests in three points were conducted at a 1 mm/min load rate using a 10 kN load cell at room temperature in an INSTRON machine, model TTDM/L. The test aimed to

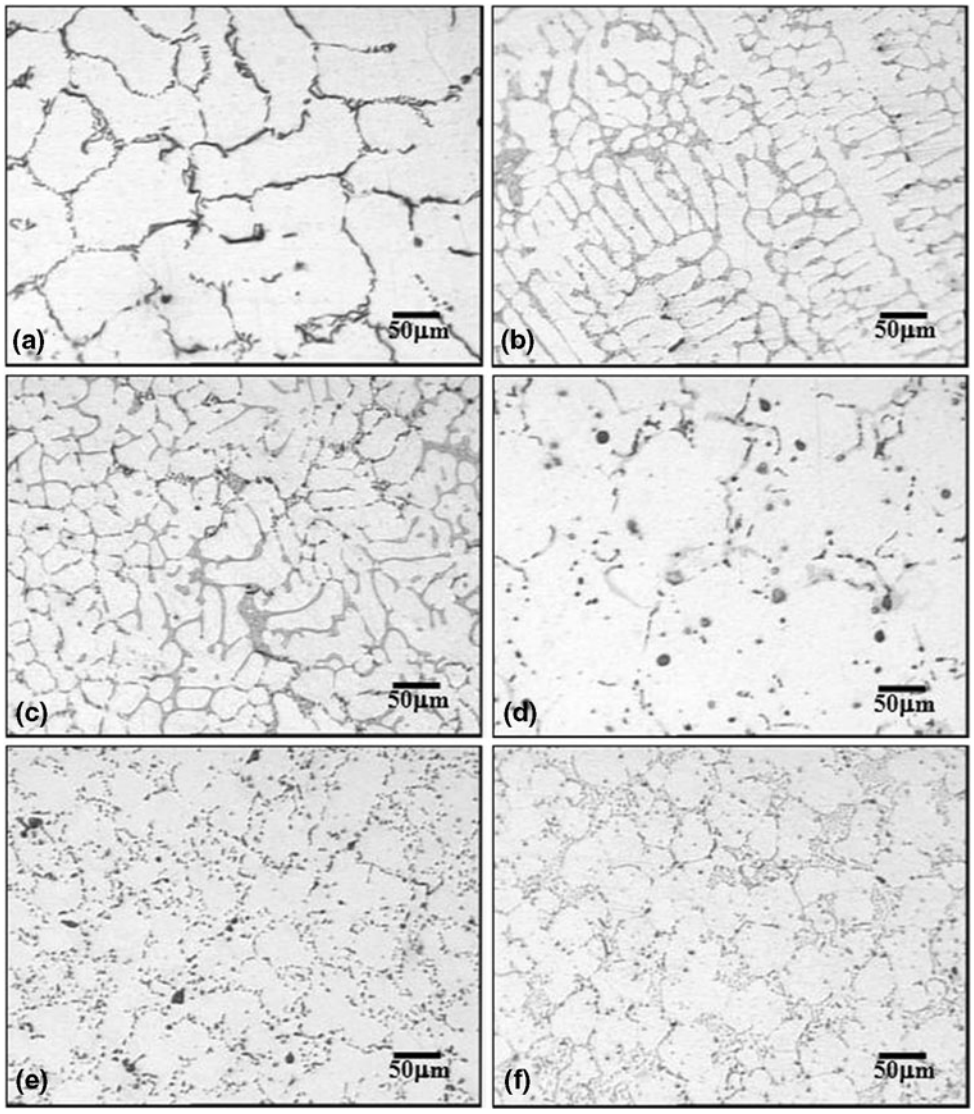

Fig. 3 Micrographs of as-cast samples of the following alloys: (a) C1, (b) C2, (c) C3, (d) C1*, (e) C2*, and (f) C3*

compare the studied alloys in terms of maximum stress by bending, σ_f, correlating them to the acquired microstructures in as-cast and annealed materials. The test specimen is shown in Fig. 2(c), and four specimens of each alloy were tested.

Rockwell C hardness tests were performed in a Hardness Test Leco RT-240 device, with a 150 kgf load and a cone-shaped diamond claw with a 120° angle. The samples for the hardness test were taken from the specimens tested in impact, and six specimens of each alloy were tested.

2.5 Fractographic and Metallographic Analyses

Metallographic analyses were performed in samples of the specimens already tried in a Zeiss microscope, model Axiotec, equipped with a Sony DXC-151 camera, connected to a Macintosh microcomputer running an image-acquiring program called Graffitek. This device provided the digital acquired images and showed the microstructures of each studied alloy. Samples were inserted in the bakelite, respectively, polished with sandpapers with granulometry #80, 120, 220, 320, 400, 600, and 1200, polished with 1.0 and 0.3 μm alumina, water-diluted, and etched with a mix of 50% picric acid diluted in alcohol and two parts of hydrofluoric acid, for 6-8 s.

The analyses by an electronic scanning microscope were performed in a Carl Zeiss SMT AG Company microscope, model LEO-440, with a potential difference from 0 to 40 kV and typical vacuum of approximately 10^{-6} Torr. The microstructure of each alloy was also evaluated after annealing to verify the effects of the treatment. A characterization by energy dispersive x-ray spectroscopy was made aiming to determine the chemical composition of the precipitated particles.

3. Results and Discussion

The weight percentage of carbon used in the chemical compounds showed to be suitable to acquire graphite in small flakes and carbides distributed over the matrix (Fig. 3). The right choice for the carbon level was fundamental to the success in obtaining good-quality test specimens, avoiding cracks and porosity as it can be observed in the Fig. 4. The specimens

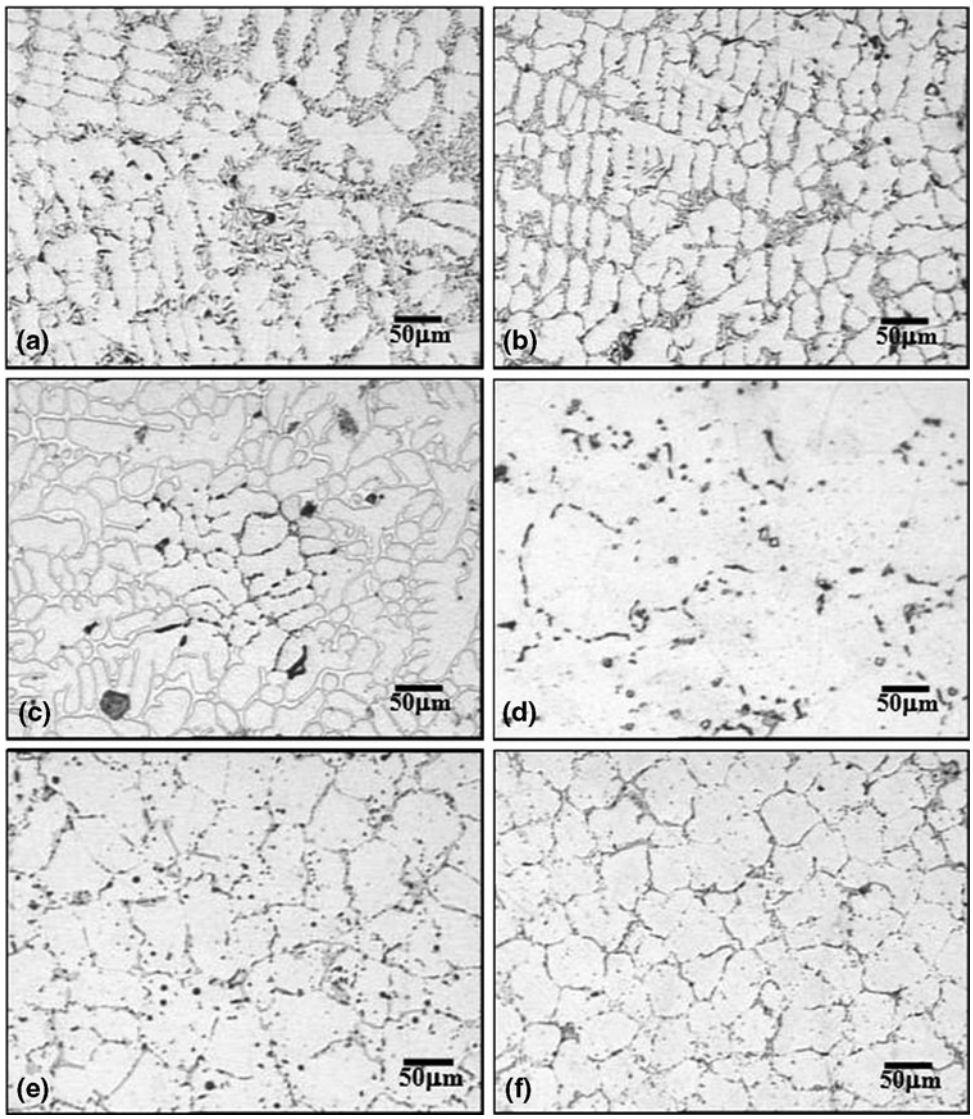

Fig. 4 Micrographs of annealed samples of the following alloys: (a) C1, (b) C2, (c) C3, (d) C1*, (e) C2*, and (f) C3*

were defect-free, although defects, such as inclusions, cracks, and bubbles, among others are common. The use of green sand in the molds did not generate any problem related to humidity. Figures 5 and 6 shows the micrographs of each studied condition: as-cast and after annealing, respectively.

Table 2 shows the results of the mechanical tests performed. The results are divided into two conditions: as-cast and annealed specimens. An increase in the mechanical properties was observed as the chromium level was increased. An increment in the mechanical strength properties was also noticed when titanium and magnesium were removed from the alloys, which is also interesting from the perspective of simplifying the process.

As-cast and titanium and magnesium-free C1, C2, and C3 alloys presented dendritic microstructures with a refined graphite distribution, as seen in Fig. 5(a)-(c), respectively. The flakes concentrate stress in the borders, decreasing the mechanical strength. After annealing heat treatment (Fig. 6a-c), a decrease was observed in the hardening figures of alloys C1, C2, and C3, according to Table 2, and a growing and coarse graphite flake formation spread among the dendritic gaps, promoting a decrease in the mechanical properties of the material. The addition of titanium and magnesium to similar alloys (C1*, C2*, and C3*) also promoted a decrease in the mechanical properties when compared to the alloy without these elements (C1, C2, and C3).

In alloy C1*, it was possible to observe the Fe + Fe_3Si_2 + C complex carbide and titanium carbide (TiC) formation homogeneously distributed in the matrix and among the dendritic gaps, as shown in Fig. 3(d). The most absorbed energy found in the as-cast material with titanium and magnesium (alloy C1*) was due to a higher strength promoted by the formed carbides, to the detriment of the graphite flakes of the as-cast material without titanium and magnesium.

Regarding alloys C1 and C1*, the heat treatment promoted a larger fine carbide precipitation, formed complex net-like structures in the dendritic gaps, increased the embrittlement, and decreased the mechanical strength for both alloys. The absorbed energy in the impact was also higher in the annealed alloy C1* than in the annealed alloy C1, as the strength promoted by the carbides is higher than the one promoted by the rough graphite flakes.

Concerning alloys C2 and C2*, as shown in Table 2, the mechanical test results and hardness measurements showed that these alloys present superior mechanical strength properties than C1 and C1* alloys, in which there was no presence of chromium, for any studied condition. Both as-cast and annealed C2 alloy presented a dendritic microstructure with complex net-like Fe + Fe_3Si_2 + C carbides, responsible for higher tensile strength. However, the annealed C2 alloy did not present chromium carbides, and the Cr remained in solid solution in the matrix.

Still regarding alloys C2 and C2*, the annealing heat treatment promoted the solubility of the iron and silicon carbides and the formation of larger coarse graphite flakes with acicular edges, concentrating strain and decreasing the mechanical strength when compared to the as-cast material, as shown in Fig. 6(b) and (c). The microstructure of the as-cast C2* alloy with titanium and magnesium is observed in Fig. 3(e), which also depicts the Fe + Fe_3Si_2 + C carbides formation finely distributed in the matrix along with the titanium carbides. The presence of chromium carbides was not observed under this

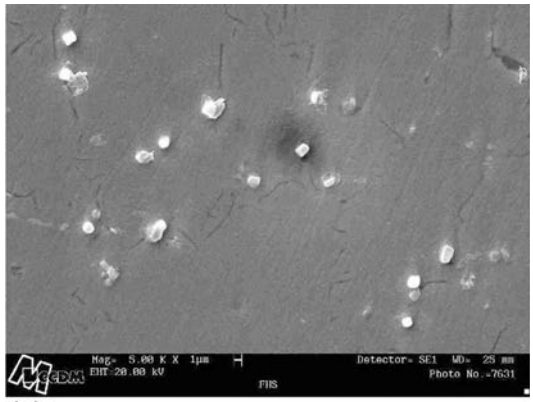

(a)

MEM1: fhs . 1
Livetime = 100 s

WINDOW LABEL	START keV	END keV	WIDTH CHANS	GROSS INTEGRAL	NET INTEGRAL	EFF. FACTOR	%AGE TOTAL
C Ka	.22	.30	5	3246	1131	1.00	3.5
MgKa	1.20	1.28	5	1635	28	1.00	.0
AlKa	1.42	1.52	6	2371	118	1.00	.3
SiKa	1.68	1.78	6	11886	3945	1.00	12.2
S Ka	2.24	2.36	7	14619	3318	1.00	10.2
TiKa	4.42	4.56	8	28859	11279	1.00	34.9
MnKa	5.80	5.96	9	1548	221	1.00	.6
FeKa	6.32	6.48	9	27896	12223	1.00	37.8

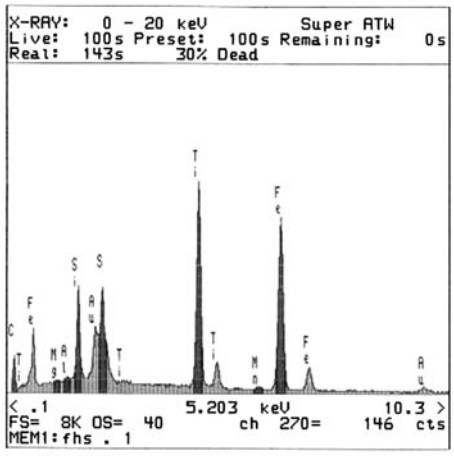

(b)

MEM1: fhs . 2
Livetime = 100 s

WINDOW LABEL	START keV	END keV	WIDTH CHANS	GROSS INTEGRAL	NET INTEGRAL	EFF. FACTOR	%AGE TOTAL
C Ka	.22	.30	5	1969	762	1.00	2.51
AlKa	1.42	1.52	6	1537	130	1.00	.43
SiKa	1.68	1.78	6	14817	5958	1.00	19.67
MnKa	5.80	5.96	9	1590	240	1.00	.79
FeKa	6.32	6.48	9	50762	22912	1.00	75.63
CuKa	7.94	8.12	10	1475	295	1.00	.97

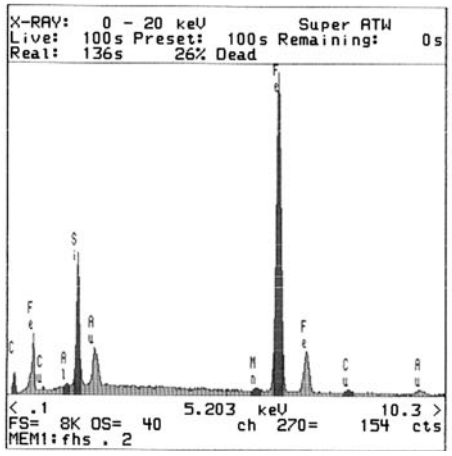

(c)

Fig. 5 (a) SEM evaluation of C1* and chemical composition determination by EDS, points (b) 1 and (c) 2

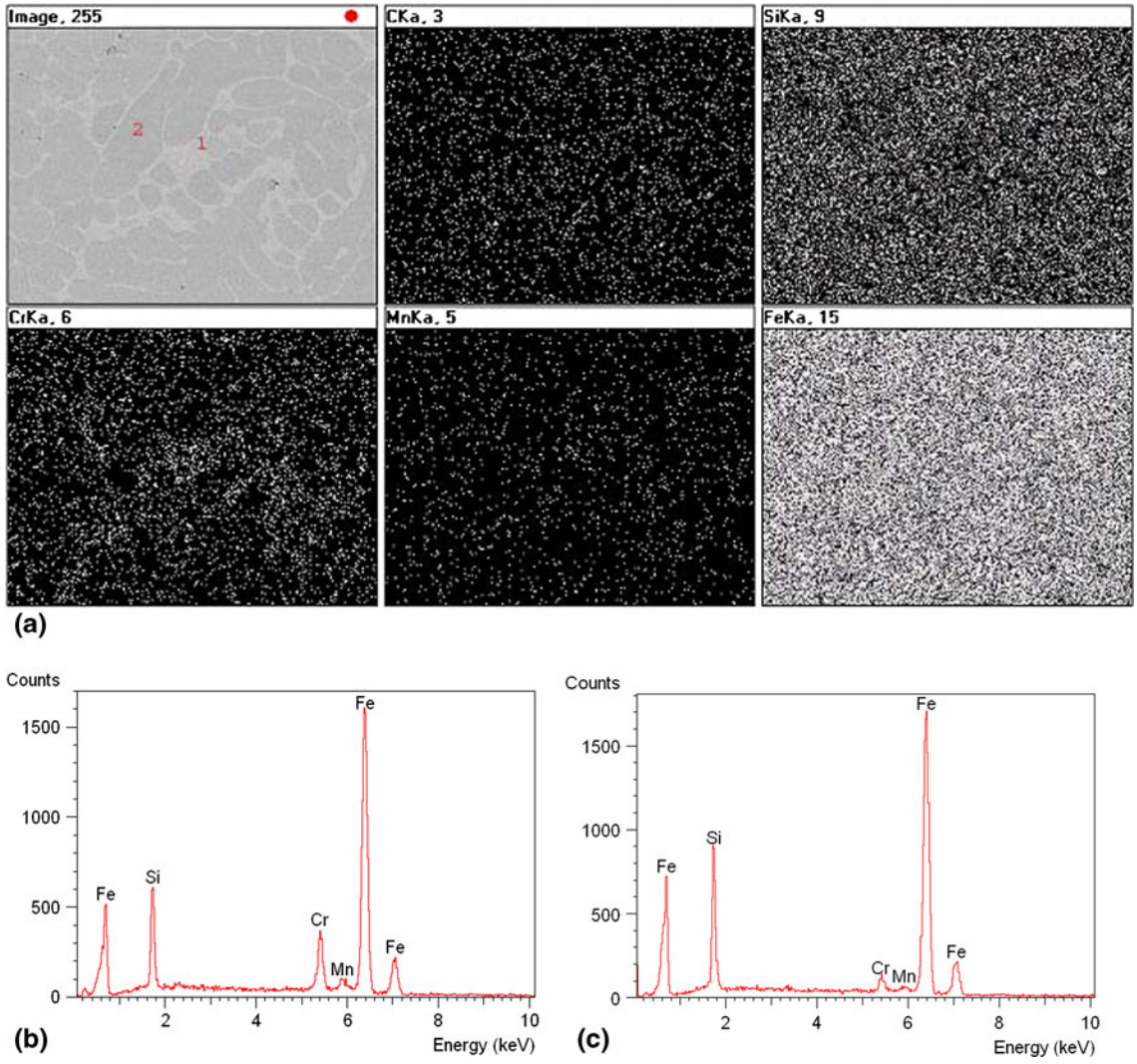

Fig. 6 Microanalysis of alloy C3*: (a) mapping of EDS alloy elements; EDS points (b) 1 and (c) 2

Table 2 Mechanic properties of the studied alloys in the states: fusion rough and annealed

	Hardness, HRC		σ_u, MPa		σ_f, MPa		Absorbed energy, J	
	As-cast	Annealed	As-cast	Annealed	As-cast	Annealed	As-cast	Annealed
C1	42 ± 1	38 ± 3	49 ± 7	35 ± 2	124 ± 2	117 ± 3	0.7 ± 0.1	0.5 ± 0.1
C2	46 ± 6	41 ± 2	57 ± 5	42 ± 5	129 ± 2	122 ± 2	0.8 ± 0.2	0.7 ± 0.1
C3	55 ± 5	44 ± 9	75 ± 3	54 ± 4	178 ± 2	139 ± 18	0.6 ± 0.1	0.4 ± 0.1
C1*	40 ± 3	36 ± 4	40 ± 2	33 ± 3	86 ± 3	80 ± 1	1.6 ± 0.2	0.8 ± 0.1
C2*	45 ± 3	41 ± 4	54 ± 6	39 ± 3	123 ± 3	115 ± 2	1.4 ± 0.1	1.2 ± 0.4
C3*	53 ± 3	42 ± 4	72 ± 2	54 ± 5	157 ± 6	122 ± 3	0.8 ± 0.1	0.8 ± 0.1

condition. For these alloys, the heat treatment also promoted a hardness decrease and the precipitation of chromium carbide, improving the mechanical strength properties. The annealing also promoted a decrease of complex iron and silicon carbides, which hampers the dislocation movement, leading to a mechanical strength reduction when compared to the as-cast material in this composition.

The as-cast C3 alloy without titanium and magnesium presented a dendritic microstructure with the presence of chromium carbides in complex net-like structures between the dendritic arms, as seen in Fig. 3(c). There was also a discreet presence of coarse graphite flakes, as there was not enough time during the solidification process to complete the carbide formation. The mechanical strength properties of this compound are superior to the last two compounds, confirming the increase in these properties when the chromium level was increased.

After annealing heat treatment in alloys C3 and C3*, as seen in Fig. 6(c) and (f), it was observed that, due to the hardness

decrease and the change in the chromium carbides morphology, these alloys presented a continuous and connected net-like morphology between the dendritic arms. The graphite present in the as-cast material did not dissolve, enlarging its flakes due to the energy provided by the annealing heat treatment.

For alloy C3, the impact toughness and bending strength values decreased, due to the change in the carbide morphology. Although the tensile strength was basically the same, there were no changes in the carbides size. For alloy C3*, due to the addition of titanium and magnesium, as in C2, the disappearance of chromium carbides occurred and the properties of mechanical strength decreased when compared to the as-cast material without these elements (C3 alloy). For alloy C3*, the addition of titanium and magnesium, as in C2, the disappearance of chromium carbides, and the properties of mechanical strength decreased when compared to the as-cast material without these elements (C3 alloy). It was possible to observe the formation of complex $Fe + Fe_3Si_2 + C$ carbides and titanium carbides (TiC) homogeneously distributed in the matrix and interdendritics, as shown Fig. 3(f). The heat treatment led to a hardness decrease in the material, following the tendency observed in the other alloys. There was a higher precipitation of titanium carbides and the appearance of chromium carbides in rough plates, decreasing the impact toughness. However, the change in the way the complex $Fe + Fe_3Si_2 + C$ carbides were presented (Fig. 3f) facilitates the dislocation movements and decreases the strength in the bending and tensile tests.

In short, the annealed specimens presented lower mechanical property values when compared to the as-cast specimens. Although the mechanical strength decreased, the annealing treatment is vital to extinguish internal stresses from the solidification process of cast parts, usually with more complex geometry than the specimen's. If there is no stress relief, there may be cracks in the spots presenting stresses during the processing of the pieces.

Although low, the values acquired for the impact tests are compatible with the cast iron used in industry. As previously stated, the annealing provided an additional reduction in the values of impact energy. Such a fact must be related to a larger presence of graphite flakes. However, the presence of graphite may be important to avoid cracks in the real parts, as it increases the thermal conductivity, helping to balance the temperature and decrease the stresses during the pieces cooling.

Figure 5 shows the microanalyses obtained by scanning electron microscopy (SEM) in a sample of C1* alloy, with Ti and Mg. In region 1, the Ti element was not detected, and more contents of Fe and Si were observed (matrix). At point 2, the precipitate was identified as a titanium carbide TiC, due to its form and EDS results.

After annealing, alloy C3* presented almost continuous chromium carbides distributed between the dendritic arms (Fig. 6a). The EDS chemical analysis showed the alloying elements distribution in the material. Points 1 and 2 indicate the chromium carbide and the matrix, respectively (Fig. 6b, c).

4. Conclusions

Regarding alloy C1, the heat treatment increased the embrittlement and decreased the mechanical strength and the absorbed energy by impact. However, for this type of alloy with Ti and Mg (C1* alloy), despite the mechanical strength decrease, there was a considerable tendency to increase the impact energy absorption.

For alloy C2, the presence of chromium promoted better results for the mechanical strength when compared to the material without this element (C1 alloy). The addition of titanium and magnesium (alloy C2*) decreased the mechanical strength. The heat treatment promoted a hardness decrease, but also promoted the formation of chromium carbides. However, when the titanium and magnesium elements were present (alloy C2*), the formation of chromium carbides was suppressed.

Finally, in alloy C3, the presence of high levels of chromium also increased the mechanical strength results. On the other hand, these alloys presented the lowest values in the absorbed energy by impact. It was observed that the same results were found in alloy C2, when the material was annealed and titanium and magnesium were added (alloy C2*). In other words, these change caused an inhibition of chromium carbide formation and the mechanical strength decrease.

Chromium increased the mechanical strength of the alloys, although, decreasing the impact toughness of the studied materials. The annealing heat treatment promoted mechanical stress and hardness decrease. The addition of titanium and magnesium to the alloys decreased the mechanical strength and hardness of the material, increasing the impact toughness.

The material to be used must be chosen considering its properties and the application to which it will be submitted, and the influence of each parameter on the material's properties.

Acknowledgments

The authors would like to acknowledge FAPESP for the financial support given, Fultec Inox Ltd. partnership in this project, as well as the Materials, Aeronautics and Automotive Engineering Department, Engineering School of São Carlos—USP, for granting us the use of its facilities.

References

1. J. Mechura, J. Klaban, Improving Properties of High-Silicon Iron Alloys, *Foundry Trade J.*, April, 1970, p 721–728
2. A. Reynaud, High-Chromium and High-Silicon Cast Irons, *Mater. Sel. Des.*, February, 1996, p 93–95
3. ASM International, Properties and Selection: Irons, Steels and High-Performance Alloys, 20th ed., Vol 1, Metals Handbook, 1990
4. B.H. Kim, J.S. Shin, S.M. Lee, and B.M. Moon, Improvement of Tensile Strength and Corrosion Resistance of High-Silicon Cast Irons by Optimizing Casting Process Parameters, *J. Mater. Sci.*, 2007, **42**, p 109–117
5. J. Dodd, Microstructures and Notes on Acid-Resisting High Silicon Iron Casting, *Br. Foundrym.*, 1961, **54**, p 277–279
6. M.G. Fontana, Sixth of a Series Summarizing Corrosion Data in Chart Form Presents Concentrations and Temperatures for Corrosion of High Silicon Iron by Sulfuric Acid, *Ind. Eng. Chem.*, 1952, **44**(2), p 85–88A
7. R.V. Riley, J.R. Park, K. Southwick, Cast and High Silicon Iron, *Chem. Ind.*, January, 1951, p 64
8. J.E. Hurst, High-Si Acid-Resisting Cast Iron, *Foundry Trade J.*, 1943, **2**, p 283–289
9. J.E. Hurst and R.V. Riley, The Occurrence of the Carbide Phase in High-Silicon Iron-Carbon Alloys, *J. Iron Steel Inst.*, 1944, **149**, p 213–219
10. M.G. Fontana, Corrosion of High Silicon Iron by Nitric Acid as a Function of Temperature is Summarized in Chart Form, *Ind. Eng. Chem.*, 1953, **45**(5), p 91–94A

11. S. Banerjee and R.K. Dutta, Complexometric Determination of Magnesium in Nodular Cast Iron and Alloyed Cast Iron Roll Samples, *Talanta*, 1980, **27**, p 212–213
12. J.L. Hague and J.I. Shultz, Determination of Magnesium in Cast Iron, *Foundry*, 1950, **78**(10), p 92
13. J. Berendson and G. Wranglén, Magnesium Sulphide as the Cause of the Higher Corrodibility of Nodular Cast Iron as Compared to Grey Cast Iron, *Corros. Sci.*, 1980, **20**, p 937–941
14. D. Zeng, Y. Zhang, J. Liu, H. He, and X. Hong, Characterization of Titanium-Containing Compounds in Gray Iron, *Tsinghua Sci. Technol.*, 2008, **13**, p 127–131
15. G. Cueva, A. Sinatora, W.L. Guesser, and A.P. Tschiptschin, Wear Resistance of Cast Irons Used in Brake Disc Rotors, *Wear*, 2003, **255**, p 1256–1260
16. ASTM A-518M, "Standard Specification for Corrosion-Resistant High-Silicon Iron Castings," Designation A518/518M-99, 1999, p 1–6